

Research Paper

Ubiquitin D Correlates with Disease Severity and T Cell Infiltration in Cholestasis: Evidence from Integrated Bioinformatics and Experimental Analyses

Huiwen Wang¹, Jian Zhang², Xun Huang¹✉, Shifang Peng²✉

1. Infection Control Center, Xiangya Hospital, Central South University, Changsha, China.

2. Department of Infectious Diseases, Xiangya Hospital, Central South University, Changsha, China.

✉ Corresponding authors: Shifang Peng, sfp1988@csu.edu.cn. Xun Huang, huangxun@csu.edu.cn.

© The author(s). This is an open access article distributed under the terms of the Creative Commons Attribution License (<https://creativecommons.org/licenses/by/4.0/>). See <https://ivyspring.com/terms> for full terms and conditions.

Received: 2025.07.29; Accepted: 2025.11.21; Published: 2026.01.01

Abstract

Cholestasis is a complex pathophysiological syndrome characterized by impaired bile secretion and excretion. Extensive research has revealed that Ubiquitin D (UBD) plays a pivotal role in numerous types of malignancies and benign diseases. However, the underlying involvement of UBD in cholestasis remains unclear. The aim of this study was to analyze the role of UBD in Cholestasis. Transcriptome data from cholestasis patients (GSE61260, GSE159676 and GSE183754) were obtained from the Gene Expression Omnibus (GEO) database. These datasets, along with cholestatic mouse models and clinical specimens, were utilized to evaluate hepatic UBD expression. Subsequently, immunohistochemistry and immunofluorescence staining were applied to validate the expression and localization of hepatic UBD. Moreover, the association of hepatic UBD levels with clinical parameters was evaluated using Pearson's correlation analysis. In addition, Gene set enrichment analysis (GSEA) and xCell were employed to investigate the immune-related signatures and immune cell infiltration link to UBD in cholestasis, with findings further validated through immunofluorescence staining. Finally, the association of the hepatic UBD with T cell-related chemokine and chemokine receptor was explored using Pearson's correlation analysis. The results showed that UBD was significantly and consistently upregulated in the livers across cholestasis patient transcriptomic data, experimental mouse models, and clinical specimens. Hepatic UBD levels positively correlate with the severity of cholestasis and hepatocytes are identified as the primary source of UBD in cholestatic livers. Functional enrichment analysis indicated that immune-related pathway was significantly activated in the cholestatic liver with high expression of UBD group. Moreover, hepatic UBD expression was positively associated with the infiltration of T cells and with the expression of T cell-related chemokines and chemokine receptors in cholestasis. In conclusion, UBD is a key gene associated with disease severity and T cells infiltration in cholestasis. These findings provide new insight into the key biomarker of cholestasis and further highlight that UBD might be a promising novel therapeutic target for patients with cholestasis.

Keywords: UBD, primary biliary cholangitis, primary sclerosing cholangitis, obstructive cholestasis, integrated bioinformatics, T cell

Introduction

Cholestasis is a complex clinical syndrome characterized by the excessive accumulation of intrahepatic bile acids (BAs), leading to inflammatory response-mediated liver injury that can progress to liver fibrosis, cirrhosis, and even liver failure[1]. Cholestasis results from diverse etiologies and manifests in various clinical settings, including primary biliary cholangitis (PBC), primary sclerosing cholangitis (PSC), viral hepatitis, cholelithiasis, and

other liver diseases[2]. In the current clinical practice, only ursodeoxycholic acid (UDCA) and obeticholic acid (OCA) have been authorized by the FDA for the treatment of limited types of cholestasis; however, their therapeutic efficacy and safety are less than satisfactory[3-5]. Therefore, it is worth deeply exploring the molecular mechanism underlying the pathological process of cholestasis which may provide therapeutic targets to combat this complex

disease.

Ubiquitin D (UBD), a ubiquitin-like protein, directly targets substrates and mediates ubiquitin-independent proteasomal degradation[6, 7]. UBD is widely expressed across multiple organs and regulates diverse cellular processes, including signal transduction, cell cycle progression, apoptosis, autophagy, and immune responses[8, 9]. Recently, the up-regulation of UBD in numerous types of malignancies[10-13] and other chronic benign disease[14-17] has attracted increasing attention. In the field of liver disease, elevated UBD expression drives tumor cell invasion, metastasis[18], and chemoresistance in hepatocellular carcinoma (HCC)[19, 20]. Additionally, hepatic UBD exacerbates metabolic dysfunction-associated steatotic liver disease (MASLD) by disrupting lipid metabolism. It is reported that the UBD expression is up-regulated by pro-inflammatory stimuli IFN- γ and TNF α [21], while the induced UBD can further promote inflammation[22, 23]. Although inflammation is a well-recognized hallmark of cholestasis and emerging evidence suggests a potential link between UBD and hepatic inflammatory responses[24, 25], the precise role of UBD in cholestasis remains to be elucidated.

Microarray and high-throughput sequencing technologies offer powerful tools for identifying genetic alterations and functional pathways in disease. Here, we reanalyzed transcriptomic data from the GEO database to evaluate UBD expression in cholestatic liver tissues across different etiologies. Subsequently, the hepatic expression of UBD was validated in the cholestasis mouse models and clinical liver samples. Meanwhile, the correlation of hepatic UBD levels with the severity of cholestasis in patients was analyzed. Moreover, Gene Ontology (GO) and Kyoto Encyclopedia of Genes and Genomes (KEGG) analyses were conducted to elucidate the biological differences between UBD-high and UBD-low groups. Finally, the immune profiling and experimental validation with clinical liver tissues were performed to evaluate the associations between UBD expression and immune cell infiltration. This work aimed to reveal the potential role of UBD in the progression of cholestatic liver disease, which may provide novel therapeutic targets for patients with cholestasis.

Materials and Methods

Data acquisition and identification of differentially expressed genes

Liver transcriptome datasets (GSE61260[26], GSE159676[27], and GSE183754[28]) were obtained from the Gene Expression Omnibus (GEO) database (<https://www.ncbi.nlm.nih.gov/geo/>). Differentially

expressed genes (DEGs) were identified using either the “limma” or DESeq2 package in R, with statistical significance defined as an adjusted p-value < 0.05 and | log2 fold change (FC) | ≥ 1 .

Functional enrichment analysis

Gene Set Enrichment Analysis (GSEA v4.3.3) was performed to evaluate whether predefined gene sets exhibited statistically significant and concordant differences between biological states. Reference gene sets were obtained from the Molecular Signatures Database (MSigDB v7.5.1). Functional enrichment analysis was assessed using the KEGG (C2) and Gene Ontology (GO, C5) subsets, with significance thresholds set at a false discovery rate (FDR) < 25% and a nominal p-value < 0.05.

Analysis of immune cell infiltration

The xCell algorithm was applied to transcriptomic data to analyze possible associations between the UBD mRNA levels and immune cell infiltration in cholestatic liver tissues[29].

Animal experiments

Eight-week-old male C57BL/6 mice were purchased from the Hunan Slake Jingda Laboratory Animals Co., Ltd. All mice were housed under specific pathogen-free (SPF) conditions with an environment of 12-hour light/dark cycle, 50 \pm 10% relative humidity and a temperature of 22 \pm 2°C. Mice were assigned randomly into three groups as follows: (1) the control group in which mice received only a standard chow diet without intervention; (2) the 0.1% 3,5-diethoxycarbonyl-1,4-dihydrocollidine (DDC) diet group in which mice fed a normal diet supplement with 0.1% DDC; (3) the bile duct ligation (BDL) group in which mice underwent surgical BDL procedure. All mice were euthanized after two weeks of experimentation and a portion of liver tissue was fixed in 10% neutral-buffered formalin for histological assessment while the remaining tissues were snap-frozen in liquid nitrogen and stored at -80°C for subsequent molecular analyses. All animal procedures were approved by the Institutional Animal Care and Use Committee of Xiangya Hospital, Central South University (No.202504063).

Immunohistochemical and immunofluorescence analysis

The experimental procedures for immunohistochemical staining were performed according to established protocols[5]. Briefly, the paraffin-embedded liver sections were deparaffinized and hydrated. Antigen retrieval was achieved with Tris-EDTA buffer (pH 9.0). Following the block of

endogenous peroxidase activity, sections were incubated overnight at 4°C with a primary antibody targeting UBD (1:500 dilution; Proteintech, cat#13003-2-AP, China). Detection was achieved using DAB chromogen (ZSbio, cat#SP-9000, China) with hematoxylin counterstaining. Bright-field images were acquired using a Leica DMIL LED microscope (200× magnification; Leica Microsystems, Germany).

Immunofluorescence staining assays were performed with multiplex Immunofluorescence staining kits (Abiowell, cat#AWI0690, China) according to the manufacturer's instructions. The liver sections were incubated primary antibodies, including anti-UBD antibody (1:100 dilution), anti-CD3 antibody (1:50 dilution; Santa Cruz, cat#sc-20047, USA), anti-ALB antibody (1:100 dilution; Abiowell, cat#AWA11256, China), anti-CK19 antibody (1:100 dilution; Abcam, cat#ab52625, USA), anti- α SMA antibody (1:100 dilution; Abcam, cat#ab124964, USA) at room temperature for 60 min. After washing, sections were probed with HRP-conjugated IgG at RT for 30 min and reacted with fluorophore-conjugated tyramine molecules for 15 min. Nuclear counterstaining was performed using DAPI for 5 minutes. Fluorescence images were captured on a ZEISS LSM880 confocal microscope (200× magnification; Carl Zeiss AG, Oberkochen, Germany). Quantitative analysis was performed on three randomly selected fields per section using Image-Pro Plus 6.0 software (Media Cybernetics, Rockville, USA). The immunoreactive area was calculated as the percentage of positive staining relative to the total tissue area.

RNA extraction and RT-qPCR analysis

Total RNA was extracted from mouse liver tissues using TRIzol reagent (Invitrogen, USA). Complementary DNA (cDNA) was then synthesized from the extracted RNA using the PrimeScript RT reagent kit (TaKaRa, Japan) according to the manufacturer's protocol. Quantitative PCR (qPCR) amplification was performed using SYBR Green Premix Ex Taq (Takara, Japan) on a Light Cycler 480 system (Roche, Switzerland). Relative gene expression quantification was determined through the comparative Ct ($2^{-\Delta\Delta Ct}$) approach, with GAPDH serving as the reference gene. The primers employed were as follows: GAPDH, forward, aggtcggtgtgaacggattttg; GAPDH, reverse, tggtagcatgtagttgaggtca; UBD, forward, ccaatggcgggtaaatgacctt; UBD, reverse, ttctgatggggccttgaggatt.

Western blot analysis

Hepatic proteins were extracted from mouse

liver samples using RIPA buffer supplemented with protease inhibitors (Roche, USA). Protein quantification was performed using a BCA assay. For immunoblotting, 30 μ g of protein per sample was separated by 10% SDS-PAGE gels and transferred onto nitrocellulose membranes. The membranes were blocked with 5% non-fat milk in TBST for 30 minutes and then incubated overnight at 4°C with primary antibodies, including anti-UBD (1:1000 dilution) and anti-GAPDH (1:1000 dilution; Abcam, cat# ab181602, USA). Following HRP-conjugated secondary antibody incubation for 1h at room temperature (RT), protein bands were visualized using enhanced chemiluminescence (ECL; Santa Cruz, USA) and quantified using ImageJ software. GAPDH served as the loading control for UBD normalization.

Patients and tissue samples

Paraffin-embedded liver sections were obtained from Xiangya Hospital (Changsha, Hunan, China) between 2017 and 2025. The cohort included samples from 7 healthy control (HC), 8 patients with PBC, 4 with PSC and 9 with obstructive cholestasis (OC). Diagnoses of PBC, PSC, and OC were established by experienced hepatologists through comprehensive clinical evaluation, including assessment of symptoms, biochemical markers, radiology, and histopathological examination of biopsied liver tissues. The control liver sections were derived from histologically normal liver tissues without pathological alterations. The detailed clinical characteristics of the enrolled patients are listed in Supplementary Table S1. This study was approved by the Ethical Committee and Institutional Review Board of Xiangya Hospital Central South University (No.2025060952). Written informed consent was obtained from all participants.

Statistical analysis

Quantitative data are presented as mean \pm SD. All statistical analyses were performed using GraphPad Prism (version 9.1.1). Bivariate correlations were assessed using Pearson's correlation coefficient. For intergroup comparisons, we employed two-tailed independent Student's t-tests for normally distributed data and Mann-Whitney U tests for non-normally distributed variables. A significance threshold of $p < 0.05$ was considered statistically significant.

Results

UBD is an up-regulated DEGs in the livers of cholestasis

Herein, we assessed the gene expression of UBD in three cholestasis-related datasets from GEO

database. The GSE61260 dataset contains 11 liver tissue samples of PBC patients and 38 normal liver tissues of HC. The GSE159676 dataset includes 12 PSC samples and 6 HC samples. The GSE183754 dataset contains 3 OC samples and 7 HC samples. As the volcano map of DEGs and the expression analysis of UBD presented in Fig. 1, UBD is a notably elevated DEG in the liver of cholestasis with different etiology including PBC (Fig. 1A), PSC (Fig. 1B), and OC (Fig. 1C), suggesting its potential role as a common pathogenic factor in cholestasis.

Validation of UBD in cholestasis mouse models

To validate UBD expression in cholestatic livers, we constructed two well-established mouse models of cholestasis: the 0.1% DDC diet-induced model which mimics the PSC pathology, and the BDL model that induces OC. H&E staining showed the marked hepatic inflammation in both models, with the distinct porphyrin deposition in the DDC model and characteristic necrotic lesions in the BDL model (Fig. 2A). immunohistochemical staining revealed that UBD protein was rarely expressed in healthy livers but highly elevated in cholestatic livers (Fig. 2A). Consistent with these findings, both qPCR and Western blot demonstrated that the mRNA and

protein expression of UBD were significantly increased in the liver of cholestasis mouse model compared to controls (Fig. 2B & C).

Intrahepatic UBD expression correlated with disease severity of cholestasis patients

To evaluate the expression of UBD in patients with cholestasis, liver tissue samples of 7 HCs, 8 patients with PBC, 4 patients with PSC and 9 patients with OC were collected. The clinical characteristics of study subjects were summarized in Table 1. Consistent with the findings in mouse models, the IHC staining confirmed significantly elevated UBD protein levels in all three cholestatic conditions (PBC, PSC, and OC) compared to healthy controls (Fig. 3A). Notably, the intrahepatic UBD levels were markedly associated with the clinicopathological features. Regression analysis demonstrated significant positive correlations between UBD expression and serum levels of ALT ($R = 0.2084$, $P = 0.0375$), ALP ($R = 0.2965$, $P = 0.0029$), TBA ($R = 0.3853$, $P = 0.0027$) and TBIL ($R = 0.2208$, $P = 0.0316$) (Fig. 3B). These results indicated that UBD is a consistently upregulated protein in human cholestasis and the expression levels of UBD is significantly associated with the severity of cholestasis.

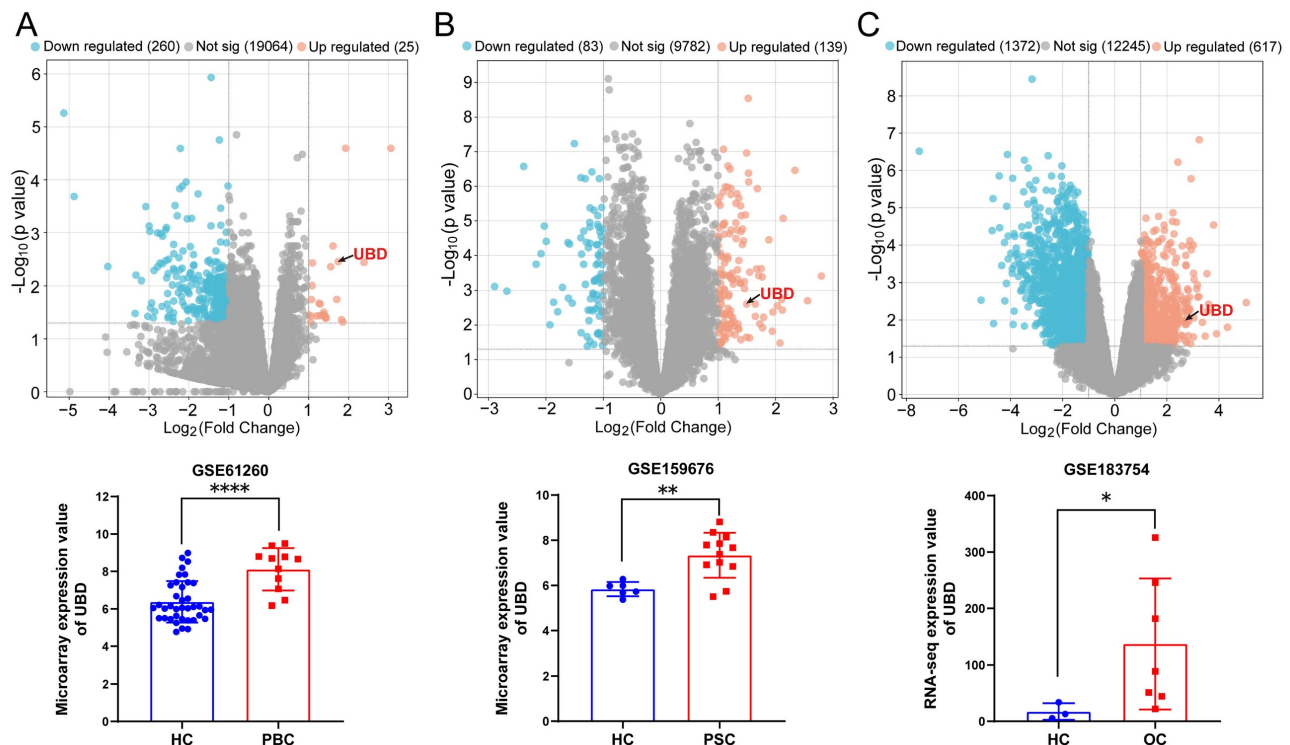


Figure 1. The expression changes of UBD between cholestasis and HC samples based on the GEO dataset. Volcano map of DEGs and the expression value of UBD in cholestasis related GEO dataset including GSE61260 (A), GSE159676 (B) and GSE183754 (C). * $p < 0.05$, ** $p < 0.01$, *** $p < 0.001$. UBD, Ubiquitin D; HC, healthy control; PBC, Primary biliary cholangitis; PSC, Primary sclerosing cholangitis; OC, Obstructive cholestasis; DEGs, differentially expressed genes; GEO, Gene Expression Omnibus.

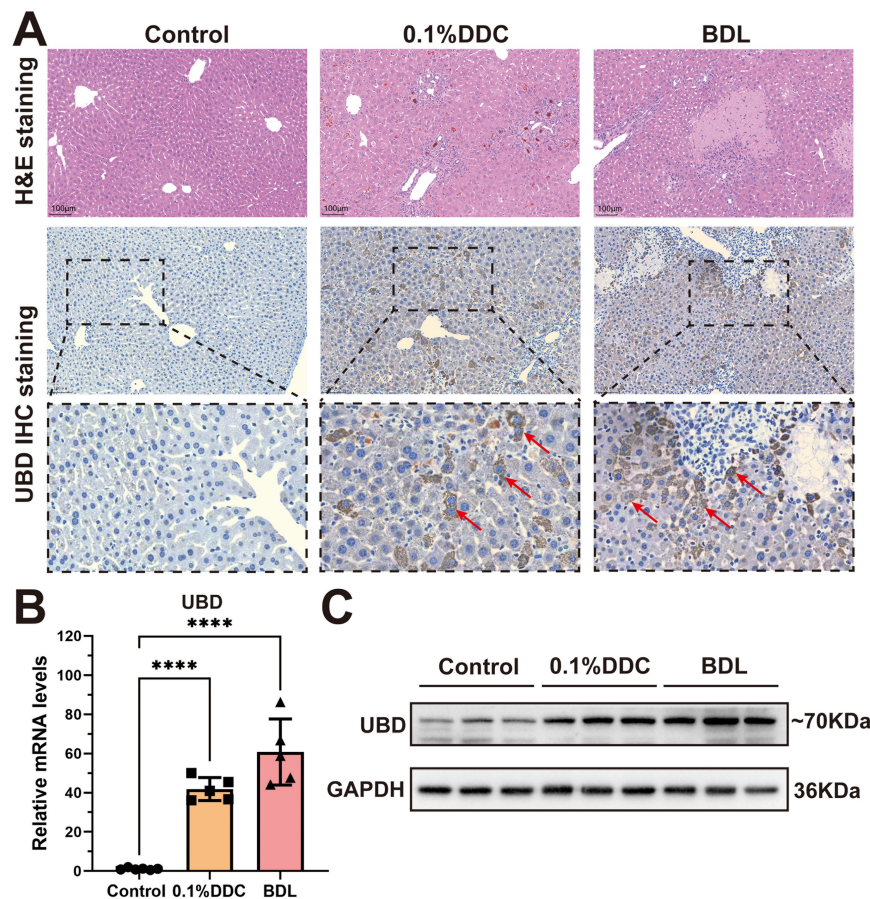


Figure 2. Histological staining and expression analysis of UBD from control and cholestatic mouse livers. (A) Representative H&E staining and UBD IHC staining images of mouse livers from control and cholestasis mice (including 0.1%DDC and BDL). (B) RT-qPCR analyses of UBD mRNA levels in livers of control and cholestasis mice. (C) Western-blot analyses of UBD protein levels in livers of control and cholestasis mice. **** $p < 0.0001$. UBD, Ubiquitin D; IHC, Immunohistochemistry; H&E, Hematoxylin and eosin; DDC, 3, 5-Diethoxycarbonyl-1,4-dihydroxycholellidine. BDL, Bile duct ligation.

Table 1. Clinical Features of Patients

Clinical Features	HC	PBC	PSC	OC
Total samples (Male/Female)	7(2/5)	8(1/7)	4(2/2)	9(4/5)
Age (years)	53.0 ± 2.0	54.0 ± 4.8	52.0 ± 10.8	58.0 ± 4.8 *
ALT (IU/L)	11.7 ± 3.1	83.1 ± 68.9 *	54.9 ± 46.9	162.4 ± 125.8 *
AST (IU/L)	17.4 ± 2.3	120.9 ± 81.2 *	67.4 ± 28.2 *	197.9 ± 160.1 *
ALP (IU/L)	79.9 ± 9.7	340.2 ± 174.6 *	147.8 ± 66.4	267.6 ± 185.8 *
GGT (IU/L)	14.1 ± 13.2	442.1 ± 444.7	226.0 ± 187.2	306.9 ± 273.6 *
TBA (µmol/L)	5.1 ± 4.1	97.4 ± 65.9 *	40.0 ± 36.4 *	78.6 ± 82.8 *
TBIL (µmol/L)	9.1 ± 2.3	167.3 ± 285.0	74.1 ± 101.8	155.4 ± 166.4 *
DBIL (µmol/L)	3.2 ± 1.5	89.3 ± 130.4	45.6 ± 69.1	92.0 ± 99.8 *

Values are means ± SD. * $P < 0.05$. Comparisons between groups were made using the two-tailed Student's t-test. Abbreviations: HC, healthy controls; PBC, primary biliary cholangitis; PSC, primary sclerosing cholangitis; OC, obstructive cholestasis; ALT, alanine aminotransferase; AST, aspartate aminotransferase; ALP, alkaline phosphatase; GGT, gamma-glutamyl transferase; TBA, total bile salts; TBIL, total bilirubin; DBIL, direct bilirubin.

UBD is specifically expressed in the hepatocytes of cholestatic livers

To further explicit the expression pattern of UBD in the different cell types of cholestatic livers, the immunofluorescence staining on liver sections of cholestasis patients was performed. Co-localization

studies with albumin (ALB) demonstrated predominant UBD expression in hepatocytes (Fig. 4A). In contrast, UBD was virtually undetectable in non-parenchymal cell populations, including hepatic stellate cells (α -SMA-positive; Fig. 4B) and cholangiocytes (CK19-positive; Fig. 4C). These findings establish hepatocytes as the primary source of UBD in the liver of cholestasis.

Elevated UBD expression associated with enhanced immune cell activity in cholestasis

To investigate the potential functions of UBD in cholestasis, we stratified cholestasis samples from three datasets into UBD low- and high-expression groups based on median UBD levels. GSEA mediated enrichment analysis was performed to identify the differences of crucial pathways and biological functions between two groups. KEGG pathway analysis demonstrated consistent enrichment of six immune-related pathways in high-UBD groups across all datasets, including the primary immunodeficiency, cytokine-cytokine receptor interaction, cell adhesion molecules, chemokine signaling pathway, T cell

receptor signaling pathway and leukocyte transendothelial migration (Fig. 5A&B). GO analysis further showed that nearly all significantly enriched biological processes in high-UBD groups were related to immune cell activity, including migration, proliferation, chemotaxis, activation, and adhesion (Fig. 5A&B). These findings indicated that hepatocyte-derived UBD in cholestasis is significantly associated with the enhanced biological activity of immune cells.

Hepatic UBD expression associated with T cell infiltration in cholestatic livers

To investigate the potential impact of hepatic UBD expression on immune cell infiltration during cholestasis, the xCell analysis was performed to compare immune cell densities between UBD low-

and high-expression groups across three datasets. In the PBC cohort, the high-UBD group showed significantly increased infiltration of CD4+ T cells, CD4+ memory T cells, CD4+ effector memory T (Tem) cells, and activated dendritic cells (Fig. 6A). The PSC cohort demonstrated elevated levels of CD4+ T cells, basophils, and immature dendritic cells in high-UBD samples (Fig. 6B). Similarly, the OC cohort exhibited increased infiltration of CD4+ T cells, CD4+ memory T cells, CD8+ central memory T (Tcm) cells, and CD8+ Tem cells in the high-UBD group (Fig. 6C). Take above together, the T cells including CD4+ and/or CD8+ T cells were the major intersecting immune cell types that highly infiltrated in the UBD high-expressed group of three datasets.

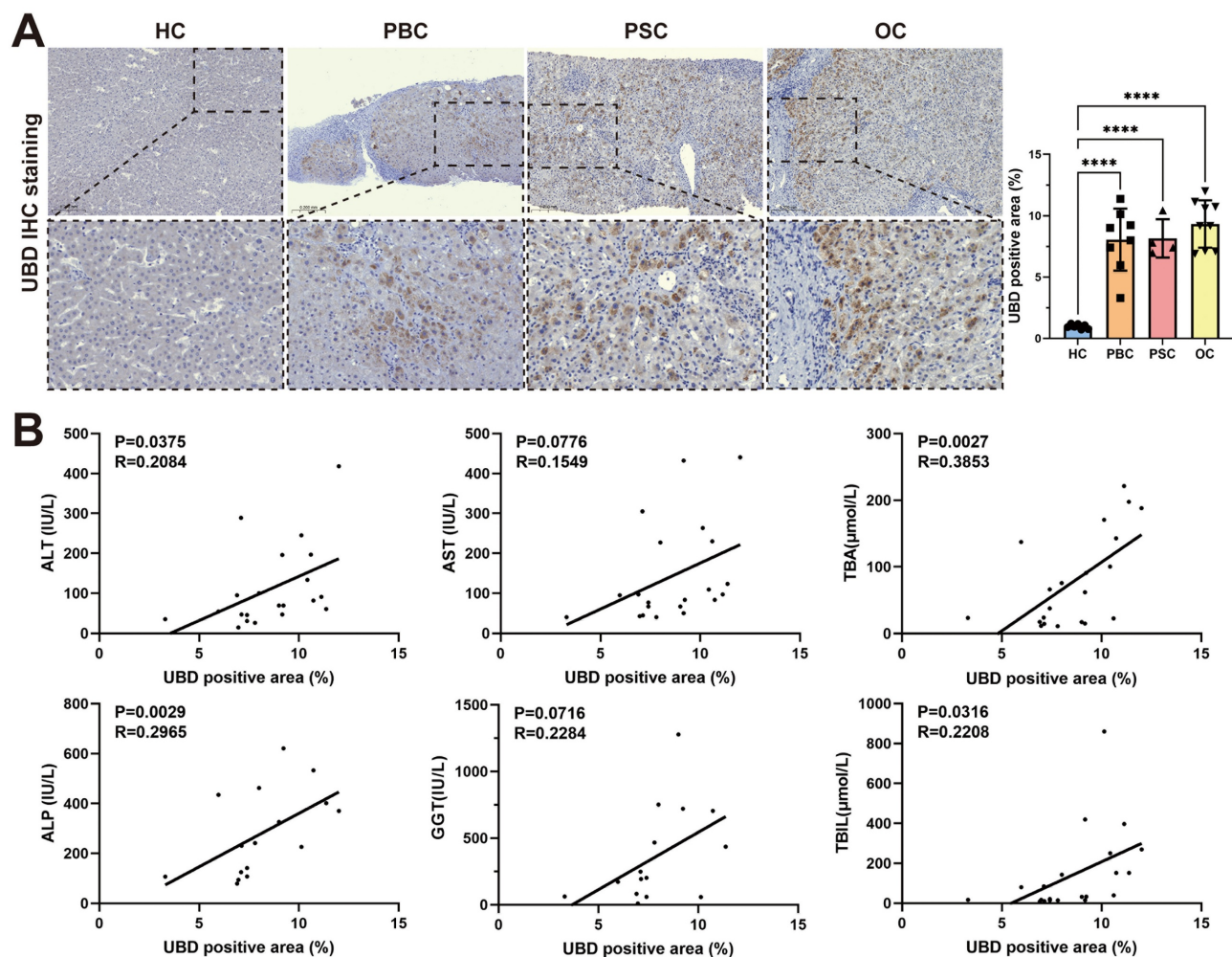


Figure 3. Validation of the intrahepatic expression of UBD and analysis of the correlation of UBD with the severity of cholestasis in patients. (A) Representative UBD IHC staining images of mouse livers from HC and patients with cholestasis including PBC, PSC and OC. (B) The relationship between intrahepatic UBD expression and clinicopathological characteristics in patients with cholestasis. **** $p < 0.0001$. UBD, Ubiquitin D; IHC, immunohistochemistry; HC, healthy control; PBC, primary biliary cholangitis; PSC, primary sclerosing cholangitis; OC, obstructive cholestasis; ALT, alanine aminotransferase; AST, aspartate aminotransferase; TBA, total bile salts; ALP, alkaline phosphatase; GGT, gamma-glutamyl transferase; TBIL, total bilirubin.

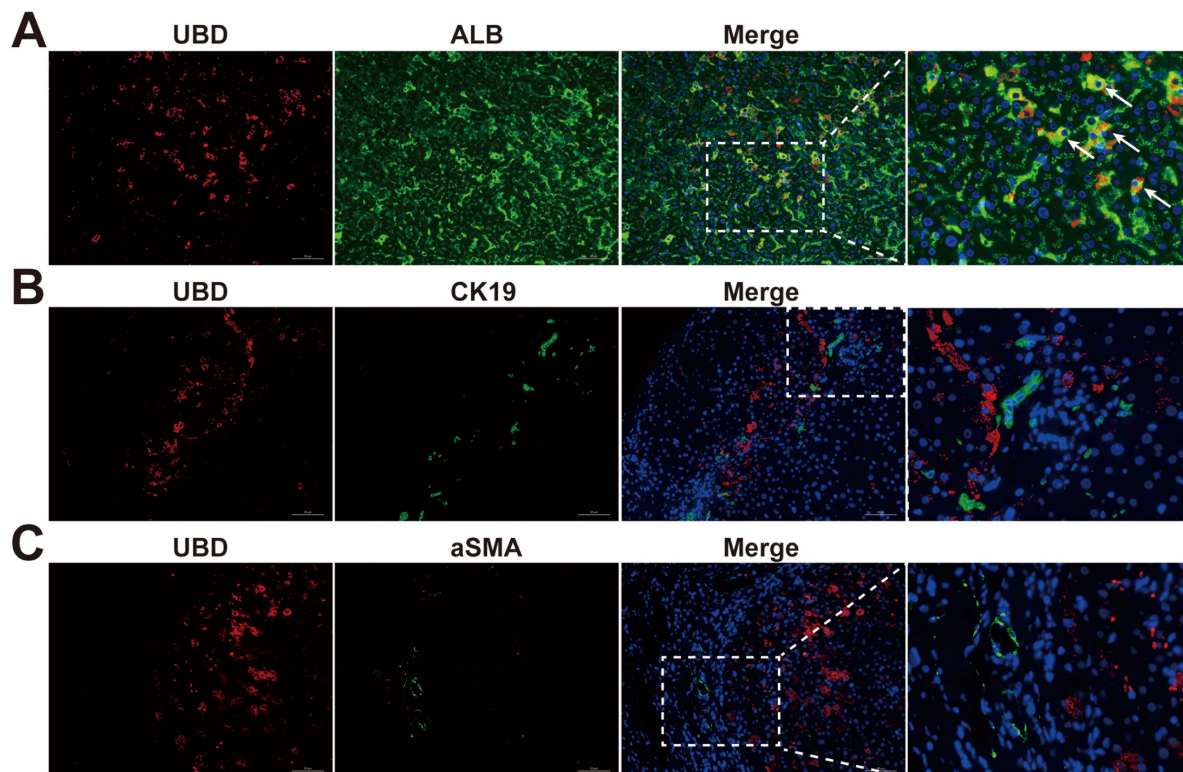


Figure 4. Localization of UBD in the livers of cholestasis patients. (A) Representative images of immunofluorescence staining for UBD (red) and ALB (green) in the liver sections from patients with cholestasis. (B) Representative images of immunofluorescence staining for UBD (red) and CK19 (green) in the liver of cholestasis. (C) Representative images of immunofluorescence staining for UBD (red) and aSMA (green) in the cholestatic liver of patients. Nuclei were labeled with DAPI (blue). UBD, Ubiquitin D; ALB, albumin; CK19, cytokeratin 19; a-SMA, α -smooth muscle actin.

To further verify the association between hepatic UBD expression and T cell infiltration, the immunofluorescence staining for the liver samples of cholestasis patients was performed. Consistent with our bioinformatic findings, the liver tissues with higher UBD expression were accompanied by more infiltration of T cells (Fig. 6D). Collectively, these results demonstrate that increased hepatic UBD expression is associated with enhanced T cell infiltration in the livers of cholestasis.

Hepatic UBD levels correlated with T cell-related chemokine and chemokine receptor expression in cholestasis

Given that T cell infiltration in cholestatic liver is mediated by chemotactic signals, we investigated potential associations between UBD expression and T cell-related chemokines/chemokine receptors. As shown in Fig. 7A, correlation analyses across PBC, PSC, and OC datasets revealed significant positive relationships between hepatic UBD expression and multiple T cell-associated chemokines (CCL18, CCL20, CCL22, CXCL10, CXCL16) as well as chemokine receptors (CCR7, CXCR4), in addition to T cell receptor subunits (CD3D, CD3E, CD3G). Specifically, in the PBC cohort, UBD levels showed

statistically significant correlations with CD3D, CD3E, CD3G, CXCL10, CCL18, CCL20, CCL22, and CXCR4 expression (Fig. 7B). The PSC cohort demonstrated significant correlations between UBD and CD3D, CD3E, CD3G, CXCL16, CCL20, CCL22, CCR7, and CXCR4 (Supplementary Fig. 1A). Similarly, the OC dataset revealed significant UBD correlations with CXCL10, CXCL16, CCL22, and CXCR4 (Supplementary Fig. 1B). These findings collectively demonstrate that hepatic UBD expression positively correlates with key T cell-recruiting chemokines and their receptors, suggesting a potential mechanism for UBD-mediated T cell migration during cholestasis.

Discussion

In the present study, through an integrated approach combining bioinformatic analysis and experimental validation, we have identified hepatic UBD as a novel key gene associated with the severity and T cell infiltration of cholestasis across multiple etiologies. The novel findings are summarized as follows: (1) Hepatic UBD expression was markedly up-regulated in both patients (PBC, PSC, and OC) and experimental mouse models (BDL and DDC-induced cholestasis); (2) Hepatic UBD expression was positively correlated with the severity of cholestasis;

(3) Hepatic UBD were positively associated with the inflammation activation, especially T-cell infiltration in cholestasis. These results established UBD as a

functionally significant mediator in cholestasis and highlighted its potential as a promising therapeutic target for cholestasis intervention.

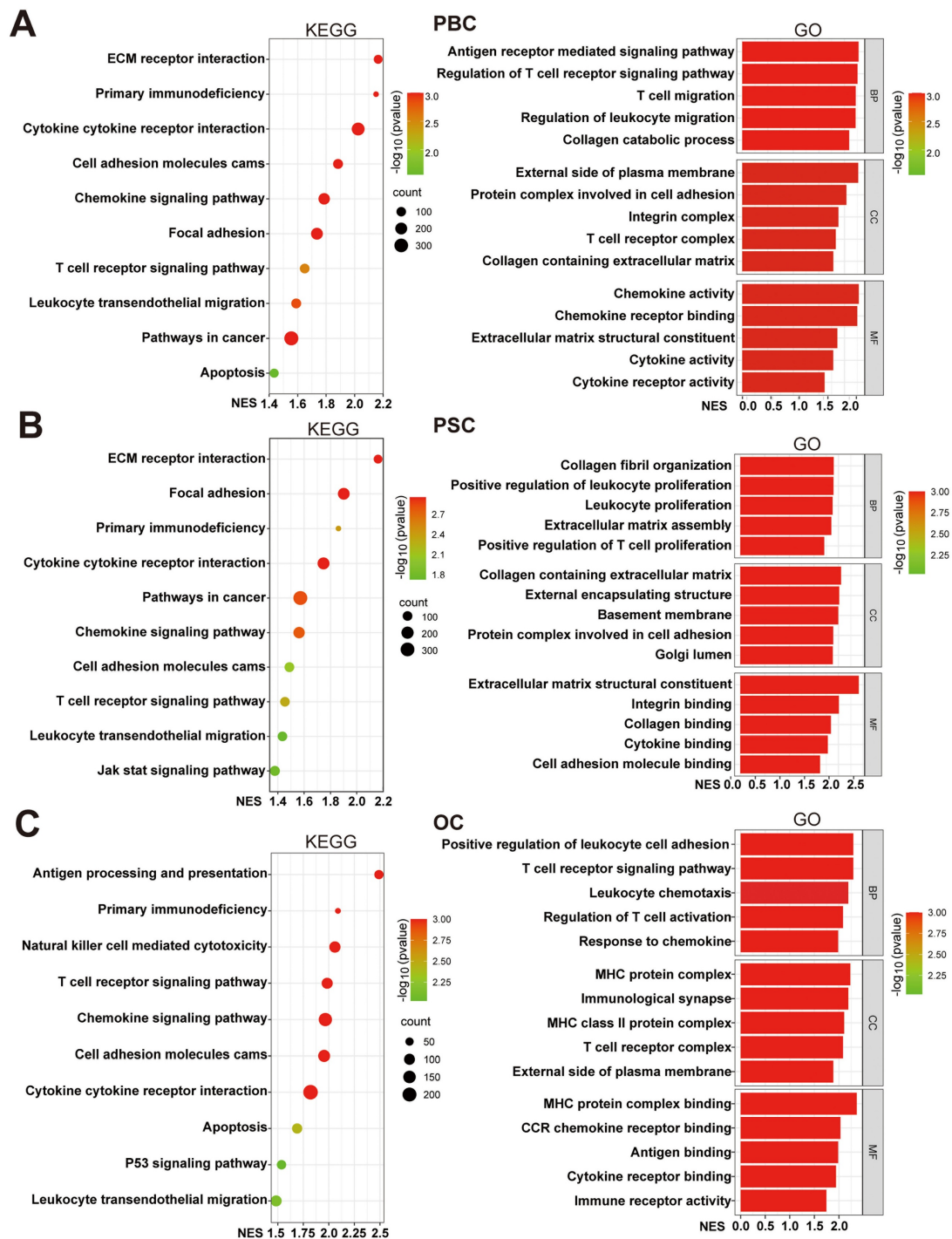


Figure 5. Functional enrichment analysis of cholestasis with high UBD levels. Cholestasis samples in the datasets were divided into UBD low and high-expressed groups based on the median expression of UBD. KEGG and GO pathways analysis of the UBD high-expression group in GSE61260 (A), GSE159676 (B) and GSE183754 datasets (C). UBD, Ubiquitin D; KEGG, kyoto encyclopedia of genes and genomes; GO, gene ontology; NES, normalized enrichment score; BP, biological process; CC, cellular components; MF, molecular function.

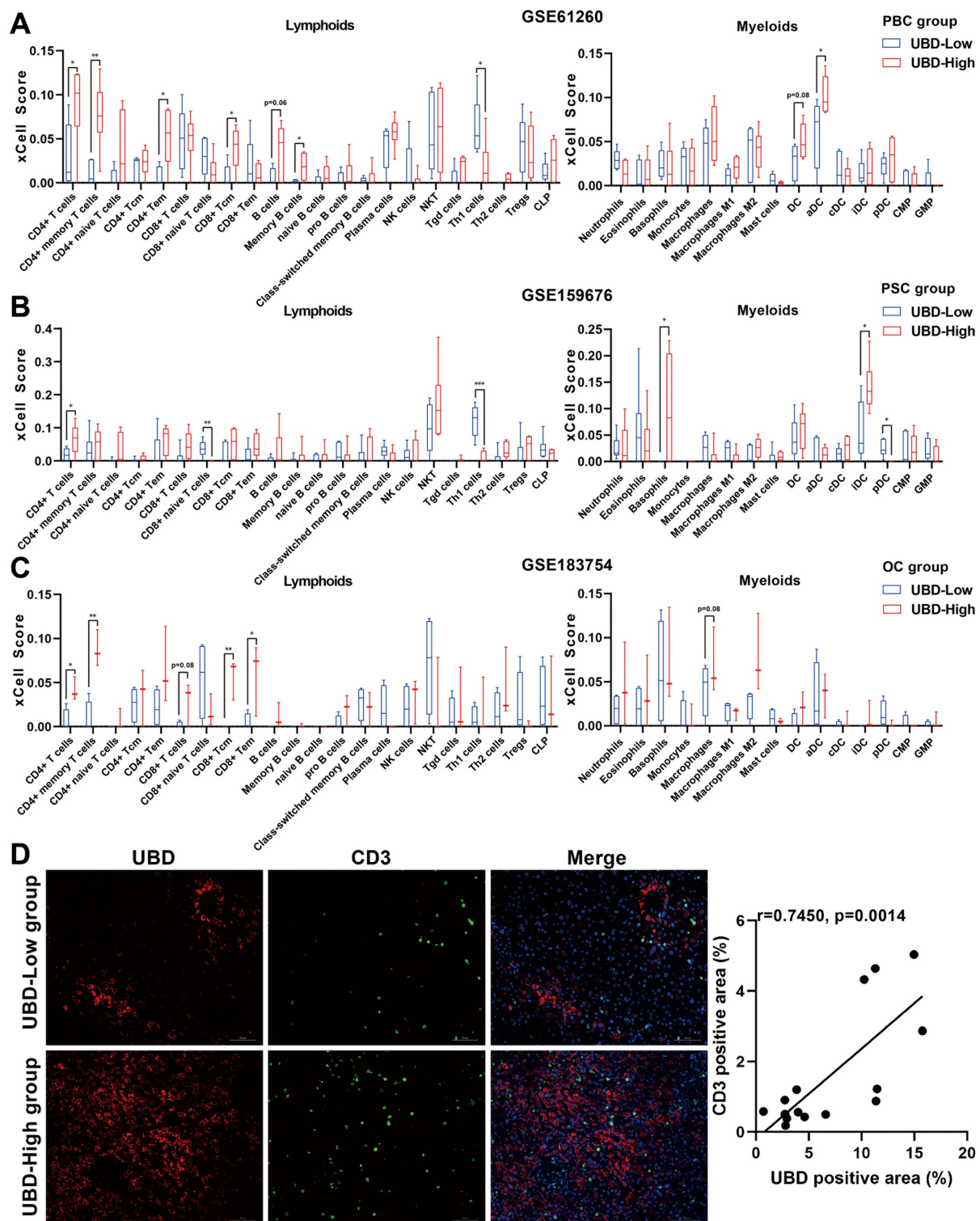


Figure 6. Relationship between hepatic UBD expression and immune cell infiltration in cholestatic livers. Infiltration of lymphoid cells and myeloid cells into cholestatic livers of the low- and high UBD groups according to xCell analysis GSE61260 (A), GSE159676 (B) and GSE183754 datasets (C). (D) Representative immunofluorescence staining images and correlation analysis of UBD and CD3-positive area in livers of cholestasis patients. * $p < 0.05$, ** $p < 0.01$, *** $p < 0.001$. UBD, Ubiquitin D.

As a member of the ubiquitin-like modifier (ULM) family, UBD classically functions to target proteins for degradation by the 26S proteasome, with UBD being degraded along with its substrates. Elevated UBD expression has been implicated in

promoting mitotic non-disjunction and chromosomal instability, suggesting a potential role in tumorigenesis. Current studies have revealed significant UBD upregulation in various cancers and non-cancer diseases[17, 30-32]. In liver disorders, the

increased hepatic UBD expression shows positive correlations with lipid accumulation in MASLD[33], enhanced invasiveness and immunosuppression in HCC[18, 19], stellate cell activation during liver fibrosis[34], and Mallory-Denk body formation in alcoholic steatohepatitis (ASH)[35]. Notably, our study provides the first evidence linking elevated hepatic UBD expression with both the severity of cholestasis and T-cell infiltration in cholestatic liver. Nevertheless, the precise function and underlying mechanisms of the upregulated UBD in the cholestasis warrant further investigation through comprehensive *in vitro* and *in vivo* studies.

Although the etiology of cholestasis varies considerably, the accumulation of bile acids in the liver represents a common pathological feature and serves as the first strike of the cholestatic liver[36]. Excessive toxic bile acids trigger hepatocytes apoptosis and inflammatory factor secretion, promote

cholangiocytes proliferation, and stimulate hepatic stellate cells activation - all of which collectively drive liver injury and fibrosis progression in cholestasis[37]. While the immune mechanisms underlying cholestasis have gradually been revealed and highlighted, they remain incompletely understood. Emerging evidence suggests that activation of resident and infiltrating immune cells, along with amplified immune responses, acts as the second hit that exacerbates cholestatic liver injury[38]. Neutrophils infiltrate during the acute phase of cholestasis[36], while other innate immune cells including macrophages, natural killer cells, and dendritic cells also participate in the cholestatic liver injury[38, 39]. Notably, adaptive immune cells - especially activated T cells - accumulate abundantly in cholestatic liver[40] and promote disease progression through cytokine release and inflammatory signaling cascade activation[38, 41]. CD8⁺ cytotoxic T

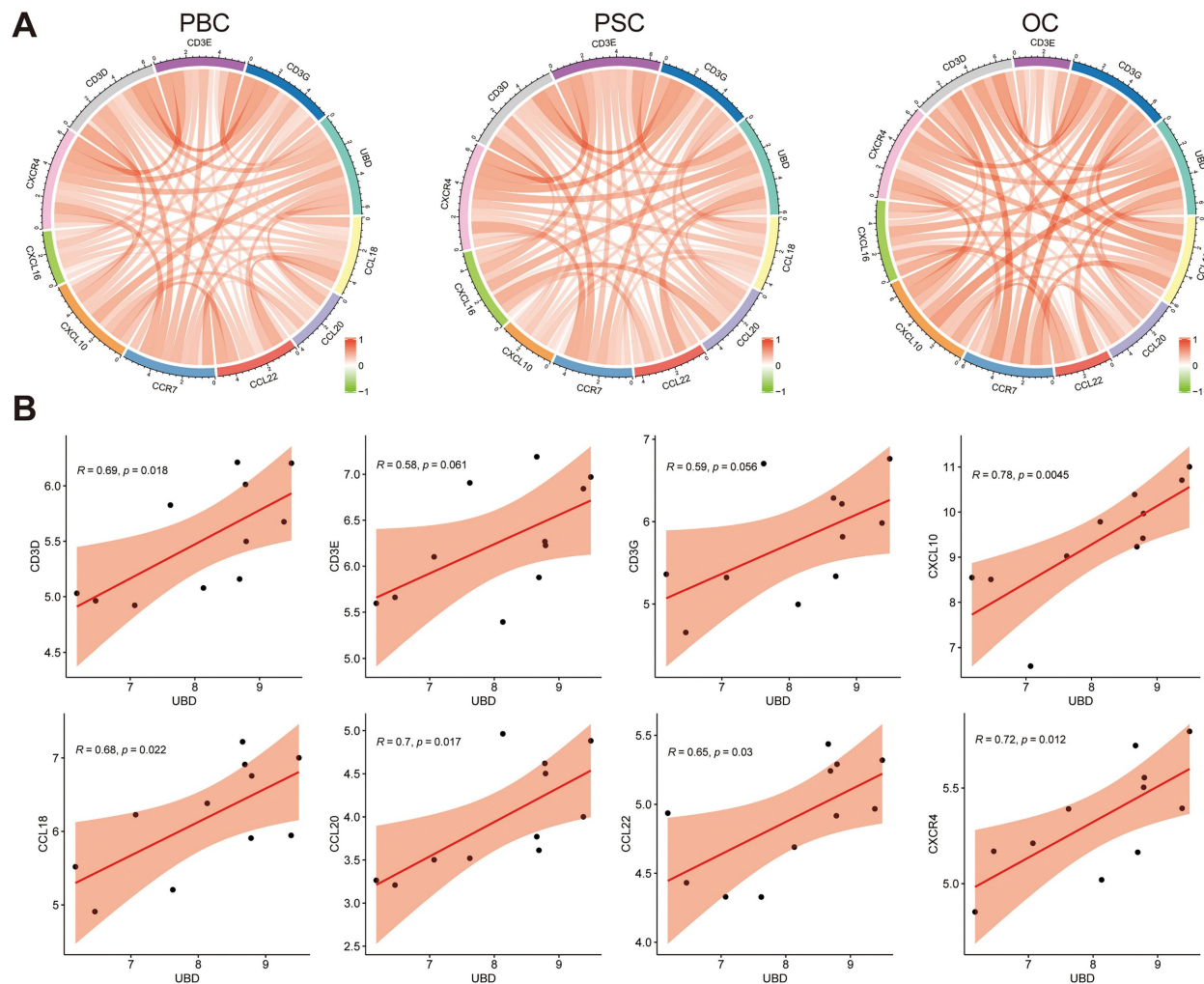


Figure 7. Relationship of UBD expression with the levels of chemokines and chemokine receptors in cholestatic livers of the datasets. (A) The circus diagram depicts Pearson correlations between UBD levels and the expression of chemokines and chemokine receptors in GSE61260, GSE159676 and GSE183754 datasets. (B) Positive correlation of UBD levels with the expression of chemokines and chemokine receptors, including CD3D, CD3E, CD3G, CXCL10, CCL18, CCL20, CCL22 and CXCR4 in GSE61260. UBD, Ubiquitin D.

lymphocytes (CTLs) are widely regarded as the primary effector cells responsible for direct bile duct epithelial cell (BEC) injury, especially in PBC. These autoreactive CD8⁺ T cells recognize specific autoantigens on BECs and induce apoptosis through mechanisms like perforin/granzyme pathways[42-44]. Concurrently, CD4⁺ T helper (Th) cells orchestrate the inflammatory microenvironment[45, 46]. The Th17 subset, in particular, has been identified as a critical pathogenic driver, especially in PSC[47]. Th17 cells, often activated by microbial-derived products from the gut, secrete pro-inflammatory cytokines such as IL-17A, which not only promote neutrophilic inflammation but also contribute directly to fibrogenesis by activating hepatic stellate cells[48-50]. Conversely, the persistence of this immunopathology is often linked to a failure in regulatory mechanisms. Regulatory T cells (Tregs), which are essential for maintaining self-tolerance, are frequently found to be numerically deficient or functionally impaired in the cholestatic liver microenvironment[51, 52]. Evidence suggests that a high bile acid milieu may destabilize the Treg phenotype, potentially skewing them towards a pathogenic Th17 profile, thus exacerbating the Th17/Treg imbalance[53]. This sustained, multifaceted T cell activation—spanning direct cytotoxicity, pro-inflammatory cytokine secretion, and pro-fibrotic signaling—is critically dependent on the chemokine gradients that recruit these subsets to the portal tracts.

It is reported that UBD induction during the maturation of the dendritic cells enhances the capacity of antigen presentation and T cell stimulation, suggesting its importance in regulating T cell activity[54]. Furthermore, elevated UBD expression correlates with increased immune cell infiltration (including T cells) in skin cutaneous melanoma[55]. In our study, we observed significant UBD induction during cholestasis (Fig. 1-3), with positive correlations to T cell infiltration (Fig. 6), as well as the expression of T cell-related chemokines and their corresponding receptors (Fig. 7). The above findings uncovered the previously unrecognized role of UBD in cholestasis. Besides, our immunofluorescence staining revealed that UBD was specifically expressed by hepatocytes rather than other nonparenchymal cells (Fig. 4). As the disorder of bile acid homeostasis initiates cholestatic liver injury, whether accumulated bile acid triggers hepatic UBD expression remains to be determined.

Several limitations should be acknowledged in this study. Firstly, further efforts are warranted for deeper mechanistic investigations of UBD in the development and progression of cholestasis.

Secondly, the potential utility of UBD as a circulating biomarker for cholestasis remains to be validated through systematic analysis of serum UBD levels in patient cohorts. Nonetheless, the findings of our study were likely reliable, as they were based on multiple datasets from patients with cholestasis, as well as experimental verification in clinical liver samples and mouse models of cholestasis with different etiologies.

Conclusion

In summary, our study identified UBD as a key gene that correlated with both cholestasis severity and hepatic T cell infiltration. These findings reveal previously unrecognized immunomodulatory functions of UBD in cholestatic liver injury, positioning it as a promising novel therapeutic target for cholestasis management.

Abbreviations

UBD: Ubiquitin; GEO: Gene Expression Omnibus; GSEA: Gene set enrichment analysis; BAs: Bile acids; HC: healthy control; PBC: Primary biliary cholangitis; PSC: Primary sclerosing cholangitis; OC: Obstructive cholestasis; UDCA: Ursodeoxycholic acid; OCA: Obeticholic acid; HCC: Hepatocellular carcinoma; MASLD: Metabolic dysfunction-associated steatotic liver disease; KEGG: Encyclopedia of Genes and Genomes; DEGs: Differentially expressed genes; GO: Gene Ontology; NES: normalized enrichment score; BP: biological process; CC: cellular components; MF: molecular function; FDR: False discovery rate; SPF: Specific pathogen-free; DDC: 0.1% 3,5-diethoxycarbonyl-1,4-dihydrocollidine; BDL: Bile duct ligation; ULM: ubiquitin-like modifier; ASH: Alcoholic steatohepatitis; IHC: Immunohistochemistry; H&E: Hematoxylin and eosin; ALT: Alanine aminotransferase; AST: Aspartate aminotransferase; TBA: Total bile salts; ALP: Alkaline phosphatase; GGT: Gamma-glutamyl transferase; TBIL: Total bilirubin; ALB: Albumin; CK19: Cytokeratin 19; α -SMA: α -smooth muscle actin.

Supplementary Material

Supplementary figure and table.

<https://www.medsci.org/v23p0350s1.pdf>

Acknowledgements

Funding

This work was supported by the National Natural Science Foundation of China (No. 82170640), the Natural Science Foundation of Changsha (Grant No. kq2502051), the Youth Science Foundation of Xiangya Hospital (Grant No. 2024Q12).

Author contributions

HW performed the experiments and wrote the manuscript. JZ collected liver tissues and clinical data and carried out the data analysis. XH and SP designed the conception of the research and revised the manuscript. All authors read and approved the final manuscript.

Ethics approval and consent to participate

The study was approved by the Ethical Committee and Institutional Review Board (No.2025060952) and the Institutional Animal Care and Use Committee (No.202504063) of Xiangya Hospital, Central South University. All authors confirmed that all methods were carried out in accordance with relevant guidelines and regulations.

Availability of data and materials

Liver transcriptome datasets GSE61260, GSE159676, and GSE183754 for this study can be found in the GEO (<http://www.ncbi.nlm.nih.gov/geo>). Further inquiries can be directed to the corresponding authors.

Competing Interests

The authors have declared that no competing interest exists.

References

- Jansen PL, Ghallab A, Vartak N, Reif R, Schaap FG, Hampe J, et al. The ascending pathophysiology of cholestatic liver disease. *Hepatology*. 2017; 65: 722-38.
- Hilscher MB, Kamath PS, Eaton JE. Cholestatic Liver Diseases: A Primer for Generalists and Subspecialists. *Mayo Clin Proc*. 2020; 95: 2263-79.
- Ge ZH, Spicer SS. Immunocytochemistry of ion transport mediators in the genital tract of female rodents. *Biol Reprod*. 1988; 38: 439-52.
- Wunsch E, Trotter J, Milkiewicz M, Raszeja-Wyszomirska J, Hirschfeld GM, Barbier O, et al. Prospective evaluation of ursodeoxycholic acid withdrawal in patients with primary sclerosing cholangitis. *Hepatology*. 2014; 60: 931-40.
- Wang H, Zhang J, Zhang X, Zhao N, Zhou Z, Tao L, et al. Fluorfenidone ameliorates cholestasis and fibrosis by inhibiting hepatic Erk1/2-Egr1 signaling and Tgfbeta1/Smad pathway in mice. *Biochim Biophys Acta Mol Basis Dis*. 2022; 1868: 166556.
- Buchsbaum S, Bercovich B, Ciechanover A. FAT10 is a proteasomal degradation signal that is itself regulated by ubiquitination. *Mol Biol Cell*. 2012; 23: 225-32.
- Aichem A, Sailer C, Ryu S, Catone N, Stankovic-Valentin N, Schmidtke G, et al. The ubiquitin-like modifier FAT10 interferes with SUMO activation. *Nat Commun*. 2019; 10: 4452.
- Fagerberg L, Hallström BM, Oksvold P, Kampf C, Djureinovic D, Odeberg J, et al. Analysis of the human tissue-specific expression by genome-wide integration of transcriptomics and antibody-based proteomics. *Mol Cell Proteomics*. 2014; 13: 397-406.
- Zhang K, Chen L, Zhang Z, Cao J, He L, Li L. Ubiquitin-like protein FAT10: A potential cardioprotective factor and novel therapeutic target in cancer. *Clin Chim Acta*. 2020; 510: 802-11.
- Chen X, Wu W, Jeong JH, Rokavec M, Wei R, Feng S, et al. Cytokines-activated nuclear IKKalpha-FAT10 pathway induces breast cancer tamoxifen-resistance. *Sci China Life Sci*. 2024; 67: 1413-26.
- Wu T, Du M, Zeng L, Wang H, Li X. Increased UBD Is a Potential Diagnostic and Prognostic Biomarker in Glioma. *Environ Toxicol*. 2024; 39: 5250-63.
- Yang Y, He R, Li D, Mu T, Kuang Z, Wang M. The pivotal role of ZNF384: driving the malignant behavior of serous ovarian cancer cells via the LIN28B/UBD axis. *Cell Biol Toxicol*. 2024; 40: 100.
- Zhu J, Zhao J, Luo C, Zhu Z, Peng X, Zhu X, et al. FAT10 promotes chemotherapeutic resistance in pancreatic cancer by inducing epithelial-mesenchymal transition via stabilization of FOXM1 expression. *Cell Death Dis*. 2022; 13: 497.
- Liu Y, Cheng K, Sun M, Ding C, Li T, Jia Y, et al. UBD participates in neutrophilic asthma by promoting the activation of IL-17 signaling. *Int J Biol Macromol*. 2024; 264: 130581.
- Shao Y, Zhang W, Du D, Yu Y, Li Q, Peng X. Ubiquitin-like protein FAT10 promotes renal fibrosis by stabilizing USP7 to prolong CHK1-mediated G2/M arrest in renal tubular epithelial cells. *Aging (Albany NY)*. 2022; 14: 7527-46.
- Xu J, Zhu L, Xu J, Lin K, Wang J, Bi YL, et al. The identification of a novel shared therapeutic target and drug across all insulin-sensitive tissues under insulin resistance. *Front Nutr*. 2024; 11: 1381779.
- Kawamoto A, Nagata S, Anzai S, Takahashi J, Kawai M, Hama M, et al. Ubiquitin D is Upregulated by Synergy of Notch Signalling and TNF-alpha in the Inflamed Intestinal Epithelia of IBD Patients. *J Crohns Colitis*. 2019; 13: 495-509.
- Yuan R, Wang K, Hu J, Yan C, Li M, Yu X, et al. Ubiquitin-like protein FAT10 promotes the invasion and metastasis of hepatocellular carcinoma by modifying beta-catenin degradation. *Cancer Res*. 2014; 74: 5287-300.
- Wang Q, Tan W, Zhang Z, Chen Q, Xie Z, Yang L, et al. FAT10 induces immune suppression by upregulating PD-L1 expression in hepatocellular carcinoma. *Apoptosis*. 2024; 29: 1529-45.
- Qiu Y, Che B, Zhang W, Zhang AV, Ge J, Du D, et al. The ubiquitin-like protein FAT10 in hepatocellular carcinoma cells limits the efficacy of anti-VEGF therapy. *J Adv Res*. 2024; 59: 97-109.
- Saxena K, Roverato ND, Reithmann M, Mah MM, Schregle R, Schmidtke G, et al. FAT10 is phosphorylated by IKKbeta to inhibit the antiviral type-I interferon response. *Life Sci Alliance*. 2024; 7.
- Gong P, Canaan A, Wang B, Leventhal J, Snyder A, Nair V, et al. The ubiquitin-like protein FAT10 mediates NF-kappaB activation. *J Am Soc Nephrol*. 2010; 21: 316-26.
- Zhuo W, Yan X, Li XQ, Chen C, Yuan P, Wan R, et al. [Effect and mechanism of ubiquitin-like protein FAT10 on Ang II induced endothelial cell inflammation]. *Zhonghua Xin Xue Guan Bing Za Zhi*. 2023; 51: 1181-7.
- Dali-Youcef N, Vix M, Costantino F, El-Saghire H, Lhermitte B, Callari C, et al. Interleukin-32 Contributes to Human Nonalcoholic Fatty Liver Disease and Insulin Resistance. *Hepatol Commun*. 2019; 3: 1205-20.
- Wimalaratne MM, Wilkerson-Vidal QC, Hunt EC, Love-Rutledge ST. The case for FAT10 as a novel target in fatty liver diseases. *Front Pharmacol*. 2022; 13: 972320.
- Horvath S, Erhart W, Brosch M, Ammerpohl O, von Schonfels W, Ahrens M, et al. Obesity accelerates epigenetic aging of human liver. *Proc Natl Acad Sci U S A*. 2014; 111: 15538-43.
- Lei L, Bruneau A, El Mourabit H, Guegan J, Folsaas T, Lemoine S, et al. Portal fibroblasts with mesenchymal stem cell features form a reservoir of proliferative myofibroblasts in liver fibrosis. *Hepatology*. 2022; 76: 1360-75.
- Gijbels E, De Muynck K, Vanderborcht B, Meese T, Van Nieuwerburgh F, Vanlander A, et al. Systematic comparison of experimental and human obstructive cholestasis reveals conservation of canonical pathway activation and biomarkers relevant for cholestatic liver disease. *Genes Dis*. 2023; 10: 18-21.
- Aran D, Hu Z, Butte AJ. xCell: digitally portraying the tissue cellular heterogeneity landscape. *Genome Biol*. 2017; 18: 220.
- Ross MJ, Wosnitzer MS, Ross MD, Graneli B, Gusella GL, Husain M, et al. Role of ubiquitin-like protein FAT10 in epithelial apoptosis in renal disease. *J Am Soc Nephrol*. 2006; 17: 996-1004.
- Baschal EE, Sarkar SA, Boyle TA, Siebert JC, Jasinski JM, Grabek KR, et al. Replication and further characterization of a Type 1 diabetes-associated locus at the telomeric end of the major histocompatibility complex. *J Diabetes*. 2011; 3: 238-47.
- Brozzi F, Gerlo S, Grieco FA, Juusola M, Balhuizen A, Lievens S, et al. Ubiquitin D Regulates IRE1alpha/c-Jun N-terminal Kinase (JNK) Protein-dependent Apoptosis in Pancreatic Beta Cells. *J Biol Chem*. 2016; 291: 12040-56.
- Clavreul L, Bernard L, Cotte AK, Hennuyer N, Bourouh C, Devos C, et al. The ubiquitin-like modifier FAT10 is induced in MASLD and impairs the lipid-regulatory activity of PPARalpha. *Metabolism*. 2024; 151: 155720.
- Zheng W, Guan F, Xu G, Yu Y, Xiao J, Huang X. FAT10 Silencing Prevents Liver Fibrosis through Regulating SIRT1 Expression in Hepatic Stellate Cells. *Int J Med Sci*. 2023; 20: 557-65.
- Jia Y, Ji P, French SW. The Role of FAT10 in Alcoholic Hepatitis Pathogenesis. *Biomedicines*. 2020; 8.
- Li M, Cai SY, Boyer JL. Mechanisms of bile acid mediated inflammation in the liver. *Mol Aspects Med*. 2017; 56: 45-53.
- Cai SY, Boyer JL. The role of bile acids in cholestatic liver injury. *Ann Transl Med*. 2021; 9: 737.
- Chen J, Zhang S. The Role of Inflammation in Cholestatic Liver Injury. *J Inflamm Res*. 2023; 16: 4527-40.
- Bernard JK, Marakovits C, Smith LG, Francis H. Mast Cell and Innate Immune Cell Communication in Cholestatic Liver Disease. *Semin Liver Dis*. 2023; 43: 226-33.
- Zimmer CL, von Seth E, Buggert M, Strauss O, Hertwig L, Nguyen S, et al. A biliary immune landscape map of primary sclerosing cholangitis reveals a dominant network of neutrophils and tissue-resident T cells. *Sci Transl Med*. 2021; 13.
- Zou M, Wang A, Wei J, Cai H, Yu Z, Zhang L, et al. An insight into the mechanism and molecular basis of dysfunctional immune response involved in cholestasis. *Int Immunopharmacol*. 2021; 92: 107328.

42. Zhu HX, Yang SH, Gao CY, Bian ZH, Chen XM, Huang RR, et al. Targeting pathogenic CD8(+) tissue-resident T cells with chimeric antigen receptor therapy in murine autoimmune cholangitis. *Nat Commun.* 2024; 15: 2936.
43. Han Y, Bian ZH, Yang SY, Wang CB, Li L, Yang YQ, et al. Single-Cell Characterization of Hepatic CD8(+) T Cells in a Murine Model of Primary Biliary Cholangitis. *Front Immunol.* 2022; 13: 860311.
44. Davies SP, Ronca V, Wootton GE, Krajewska NM, Bozward AG, Fiancette R, et al. Expression of E-cadherin by CD8(+) T cells promotes their invasion into biliary epithelial cells. *Nat Commun.* 2024; 15: 853.
45. Tanaka A, Leung PSC, Gershwin ME. Evolution of our understanding of PBC. *Best Pract Res Clin Gastroenterol.* 2018; 34-35: 3-9.
46. Andrews TS, Nakib D, Perciani CT, Ma XZ, Liu L, Winter E, et al. Single-cell, single-nucleus, and spatial transcriptomics characterization of the immunological landscape in the healthy and PSC human liver. *J Hepatol.* 2024; 80: 730-43.
47. Poch T, Krause J, Casar C, Liwinski T, Glau L, Kaufmann M, et al. Single-cell atlas of hepatic T cells reveals expansion of liver-resident naive-like CD4(+) T cells in primary sclerosing cholangitis. *J Hepatol.* 2021; 75: 414-23.
48. Nakamoto N, Sasaki N, Aoki R, Miyamoto K, Suda W, Teratani T, et al. Gut pathobionts underlie intestinal barrier dysfunction and liver T helper 17 cell immune response in primary sclerosing cholangitis. *Nat Microbiol.* 2019; 4: 492-503.
49. Kunzmann LK, Schoknecht T, Poch T, Henze L, Stein S, Kriz M, et al. Monocytes as Potential Mediators of Pathogen-Induced T-Helper 17 Differentiation in Patients With Primary Sclerosing Cholangitis (PSC). *Hepatology.* 2020; 72: 1310-26.
50. Chen W, Chen X, Gao F, Yao Q, Cheng S, Pan Q, et al. Mesenchymal stem cell-derived extracellular vesicles attenuate periductal fibrosis by inhibiting Th17 differentiation in human liver multilineage organoids and Mdr2(-/-) mice. *J Nanobiotechnology.* 2025; 23: 546.
51. Sebode M, Peiseler M, Franke B, Schwinge D, Schoknecht T, Wortmann F, et al. Reduced FOXP3(+) regulatory T cells in patients with primary sclerosing cholangitis are associated with IL2RA gene polymorphisms. *J Hepatol.* 2014; 60: 1010-6.
52. Bernuzzi F, Fenoglio D, Battaglia F, Fravega M, Gershwin ME, Indiveri F, et al. Phenotypical and functional alterations of CD8 regulatory T cells in primary biliary cirrhosis. *J Autoimmun.* 2010; 35: 176-80.
53. Kudira R, Yang ZF, Osuji I, Damen M, Yang Vom Hofe A, Singh M, et al. Bile acids engage the SLPR-STAT3 signaling axis to modulate regulatory T cell responses in fibrosing cholangiopathies. *J Hepatol.* 2025; 83: 1128-41.
54. Ebstein F, Lange N, Urban S, Seifert U, Kruger E, Kloetzel PM. Maturation of human dendritic cells is accompanied by functional remodelling of the ubiquitin-proteasome system. *Int J Biochem Cell Biol.* 2009; 41: 1205-15.
55. Wang Y, Zhang H. FAT10 is a Prognostic Biomarker and Correlated With Immune Infiltrates in Skin Cutaneous Melanoma. *Front Mol Biosci.* 2022; 9: 805887.